Segmentation of the Left Ventricle Using Distance Regularized Two-Layer Level Set Approach

Chaolu Feng[1,2], Chunming Li[2,*], Dazhe Zhao[1], Christos Davatzikos[2], and Harold Litt[3]

[1] Key Laboratory of Medical Image Computing of Ministry of Education, Northeastern University, Shenyang, LiaoNing 110819, China
[2] Center for Biomedical Image Computing and Analytics, University of Pennsylvania, Philadelphia, PA 19104, USA
Chunming.Li@uphs.upenn.edu
[3] Department of Radiology, University of Pennsylvania, Philadelphia, PA 19104, USA

Abstract. We propose a novel two-layer level set approach for segmentation of the left ventricle (LV) from cardiac magnetic resonance (CMR) short-axis images. In our method, endocardium and epicardium are represented by two specified level contours of a level set function. Segmentation of the LV is formulated as a problem of optimizing the level set function such that these two level contours best fit the epicardium and endocardium. More importantly, a distance regularization (DR) constraint on the level contours is introduced to preserve smoothly varying distance between them. This DR constraint leads to a desirable interaction between the level contours that contributes to maintain the anatomical geometry of the endocardium and epicardium. The negative influence of intensity inhomogeneities on image segmentation are overcome by using a data term derived from a local intensity clustering property. Our method is quantitatively validated by experiments on the datasets for the MICCAI grand challenge on left ventricular segmentation, which demonstrates the advantages of our method in terms of segmentation accuracy and consistency with anatomical geometry.

1 Introduction

Non-invasive assessment of left ventricular function is an important part of the diagnosis and management of cardiovascular disease. Cine MRI has been proven to be an accurate and reproducible modality for quantitative evaluation of left ventricular function [1–6]. Relevant measurements include ventricular volume, mass, and cavity ejection fraction (EF), which are based on the results of delineation of endocardial and epicardial boundaries by segmentation techniques. However, LV segmentation is still a open problem and is challenging due to poor contrast between tissues around the epicardium and intensity inhomogeneities in cine CMR images.

* Corresponding author.

K. Mori et al. (Eds.): MICCAI 2013, Part I, LNCS 8149, pp. 477–484, 2013.

Active contour models and level set methods have been extensively applied to image segmentation because they can provide smooth and closed contours as segmentation results and achieve sub-pixel accuracy for identification of object boundaries [7]. They have also been used to segment the LV in [3–6]. Zeng *et al.* proposed a coupled surfaces propagation method to extract the LV myocardium [3]. This method was further developed in [4] and [5]. In these methods, a hard constraint was imposed to force the distance between endocardium and epicardium to be within a given interval. Chung and Vese proposed a multilayer level set method to segment images by representing object boundaries as multiple level sets of a single level set function [6]. However, there is no constraint on the distance between level contours of the level set function in their method. In addition, none of the above-mentioned level set methods is able to deal with intensity inhomogeneities in the images.

In this paper, we propose a novel two-layer level set approach for segmentation of the LV from cine CMR short-axis images. In our method, the endocardium and epicardium are represented by two specified level contours of a level set function. The anatomical geometry of the LV is preserved by a distance regularization constraint on the level contours. The data term of our method, derived from a local intensity clustering property, is able to segment the images in the presence of intensity inhomogeneities [8].

2 Distance Regularized Two-Layer Level Set Method

2.1 Energy Formulation

We consider an image I as a function $I : \Omega \to \Re$ defined on a continuous domain Ω. Let $\phi : \Omega \to \Re$ be a *level set function*. We denote by C_0 and C_k the 0-level and k-level contours of ϕ, i.e. $C_0 \triangleq \{\mathbf{x} : \phi(\mathbf{x}) = 0\}$ and $C_k \triangleq \{\mathbf{x} : \phi(\mathbf{x}) = k\}$. We use the 0-level contour and k-level contour to represent the endocardium and epicardium. The contours C_0 and C_k separate the image domain Ω into three regions: $\Omega_1 \triangleq \{\mathbf{x} : \phi(\mathbf{x}) < 0\}$, $\Omega_2 \triangleq \{\mathbf{x} : 0 < \phi(\mathbf{x}) < k\}$, and $\Omega_3 \triangleq \{\mathbf{x} : \phi(\mathbf{x}) > k\}$. According to the heart anatomy, the regions Ω_1 and Ω_2 represent the cavity and myocardium, respectively, and Ω_3 the region outside the epicardium. Let H be the Heaviside function, then the membership functions of these regions can be expressed as $M_1(\phi(\mathbf{x})) = 1 - H(\phi(\mathbf{x}))$, $M_2(\phi(\mathbf{x})) = H(\phi(\mathbf{x})) - H(\phi(\mathbf{x}) - k)$, and $M_3(\phi(\mathbf{x})) = H(\phi(\mathbf{x}) - k)$, with $M_i(\phi(\mathbf{x})) = 1$ for $\mathbf{x} \in \Omega_i$ and $M_i(\phi(\mathbf{x})) = 0$ for $\mathbf{x} \notin \Omega_i$.

In the ideal case that the thickness of the myocardium is a constant, the distance between the 0-level and the k-level contours of the level set function that represent the endocardial and epicardial contours is a constant. The equal distance between these two level contours can be ensured by the constraint that $|\nabla\phi(\mathbf{x})|$ is a constant. However, the actual thickness of myocardium is primarily smoothly varying. In this case, we force $|\nabla\phi(\mathbf{x})|$ to be a smooth function $\alpha(\mathbf{x})$ by imposing a constraint on ϕ as an energy functional, defined by

$$\mathcal{R}(\phi, \alpha) = \mu \int \frac{1}{2}(|\nabla\phi(\mathbf{x})| - \alpha(\mathbf{x}))^2 d\mathbf{x} + \omega \int |\nabla\alpha(\mathbf{x})|^2 d\mathbf{x}, \tag{1}$$

where $\mu > 0$, $\omega > 0$ are the weighting coefficients. The first term forces $|\nabla\phi|$ to be a smooth function $\alpha(\mathbf{x})$, and the smoothness of $\alpha(\mathbf{x})$ is ensured by the second term. This energy $\mathcal{R}(\phi, \alpha)$ is used as the distance regularization term in conjunction with a data term and a length term, as defined below, in the proposed variational framework. It is worth noting that this DR term with $\alpha = 1$ was originally used by Li *et al.* in [9] to force the level set function to be close to a signed distance function, thereby eliminating the need for re-initialization in conventional level set methods. In this paper, the DR term is used for a different purpose, namely, to maintain smoothly varying distance between two level contours.

Note that, the distance between the 0-level and k-level contours depends on the values of k and $|\nabla\phi|$. For a given value of k, the values of $|\nabla\phi|$ can be adaptively changed in the energy minimization process, such that the distance between the 0-level and k-level contours matches the actual distance between the endocardium and epicardium. Therefore, the choice of the level k is flexible, and the result of our method is not sensitive to the choice of k. We set $k = 15$ for all the images in the experiments presented in this paper.

Due to the intensity inhomogeneities in CMR, the distributions of the intensities in the regions Ω_1, Ω_2, and Ω_3 often overlap, which is a major challenge when using intensity based segmentation methods. To overcome this difficulty, we exploit the property of intensities in a relatively small circular neighborhood, in which the slowly varying bias can be ignored. This neighborhood can be defined by $\mathcal{O}_{\mathbf{y}} \triangleq \{\mathbf{x} : |\mathbf{x} - \mathbf{y}| \leq \rho\}$. The partition $\{\Omega_i\}_{i=1}^3$ of the entire domain Ω induces a partition of the neighborhood $\mathcal{O}_{\mathbf{y}}$, i.e., $\{\mathcal{O}_{\mathbf{y}} \cap \Omega_i\}_{i=1}^3$ forms a partition of $\mathcal{O}_{\mathbf{y}}$. For the slowly varying bias, image intensities in $\mathcal{O}_y \cap \Omega_1$, $\mathcal{O}_y \cap \Omega_2$, and $\mathcal{O}_y \cap \Omega_3$ can be approximated by three constants, denoted by $f_1(\mathbf{y})$, $f_2(\mathbf{y})$, and $f_3(\mathbf{y})$. Therefore, the intensities in the set $\mathbf{I}_i^{\mathbf{y}} = \{I(\mathbf{x}) : \mathbf{x} \in \mathcal{O}_y \cap \Omega_i\}$ form a cluster with cluster center $m_i \approx f_i(\mathbf{y}), i = 1, 2, 3$. This property of local intensities directs us to apply K-means clustering to classify these local intensities. Therefore, as in [8], we define a clustering criterion for classifying the intensities in $\mathcal{O}_y$ as follows

$$\mathcal{E}_{\mathbf{y}} = \sum_{i=1}^{3} \lambda_i \int_{\mathcal{O}_y \cap \Omega_i} K_\rho(\mathbf{x} - \mathbf{y}) |I(\mathbf{x}) - f_i(\mathbf{y})|^2 d\mathbf{x} \tag{2}$$

where λ_1, λ_2, and λ_3 are the weighting coefficients and K_ρ is a kernel function $K_\rho : \Re^n \to [0, +\infty)$, defined by $K_\rho(\mathbf{u}) = a$ for $|\mathbf{u}| \leq \rho$ and $K_\rho(\mathbf{u}) = 0$ for $|\mathbf{u}| > \rho$, where $a > 0$ is a normalization factor such that $\int_{|\mathbf{u}| \leq \rho} K_\rho(\mathbf{u}) = 1$. A desired segmentation can be achieved by seeking an optimal partition $\{\Omega_i\}_{i=1}^3$ and optimal fitting functions $f_1(\mathbf{y})$, $f_2(\mathbf{y})$, and $f_3(\mathbf{y})$, such that $\mathcal{E}_{\mathbf{y}}$ is minimized for all $\mathbf{y} \in \Omega$. Since $K_\rho(\mathbf{x} - \mathbf{y}) = 0$ for $\mathbf{x} \notin \mathcal{O}_y$, we can rewrite $\mathcal{E}_{\mathbf{y}}$ as

$$\mathcal{E}_{\mathbf{y}} = \sum_{i=1}^{3} \lambda_i \int K_\rho(\mathbf{x} - \mathbf{y}) |I(\mathbf{x}) - f_i(\mathbf{y})|^2 M_i(\phi(\mathbf{x})) d\mathbf{x}, \tag{3}$$

where $M_i(\phi(\mathbf{x}))$ is the membership functions of the region Ω_i as defined earlier.

As mentioned earlier, the energy $\mathcal{E}_{\mathbf{y}}$ should be minimized for all $\mathbf{y} \in \Omega$. This can be achieved by minimizing the integral of $\mathcal{E}_{\mathbf{y}}$ with respect to the neighborhood center $\mathbf{y}$, which is the energy functional $\mathcal{E}$ defined by

$$\mathcal{E}(\phi, f_1, f_2, f_3) = \sum_{i=1}^{3} \lambda_i \int \left(\int K_\rho(\mathbf{x}-\mathbf{y}) |I(\mathbf{x}) - f_i(\mathbf{y})|^2 M_i(\phi(\mathbf{x})) d\mathbf{x} \right) d\mathbf{y}. \quad (4)$$

As in most active contour models, we smooth the contours by penalizing their lengths. Therefore, we define

$$\mathcal{L}(\phi) = \nu_1 \int |\nabla H(\phi(\mathbf{x}))| d\mathbf{x} + \nu_2 \int |\nabla H(\phi(\mathbf{x}) - k)| d\mathbf{x}, \quad (5)$$

where the first term and the second term compute the arc lengths of the 0-level and k-level contours, respectively.

With the energy terms $\mathcal{R}(\phi, \alpha)$, $\mathcal{E}(\phi, f_1, f_2, f_3)$, and $\mathcal{L}(\phi)$ defined above, we propose to minimize the following energy functional:

$$\mathcal{F}(\phi, \alpha, f_1, f_2, f_3) = \mathcal{R}(\phi, \alpha) + \mathcal{E}(\phi, f_1, f_2, f_3) + \mathcal{L}(\phi). \quad (6)$$

2.2 Energy Minimization

Minimization of the energy $\mathcal{F}(\phi, \alpha, f_1, f_2, f_3)$ can be achieved by alternately minimizing $\mathcal{F}$ with respect to each of its variables. The energy minimization process starts with an initialization of the level set function ϕ and the smooth function α. The smooth function α can be initialized as a constant function, i.e. $\alpha = c$ with $c > 0$ being a constant. After a number of iterations of the level set function, the function is updated as the minimizer of the energy $\mathcal{R}(\phi, \alpha)$ given the updated ϕ in previous iteration. The minimization of $\mathcal{R}(\phi, \alpha)$ with respect to α can be achieved by solving the gradient flow equation derived from the energy $\mathcal{R}(\phi, \alpha)$, which is a standard heat equation. The heat equation can be solved approximately by a convolution of the function $|\nabla\phi|$ with a Gaussian kernel. For a fixed level set function ϕ, we minimize $\mathcal{F}(\phi, \alpha, f_1, f_2, f_3)$, or equivalently minimize $\mathcal{E}(\phi, f_1, f_2, f_3)$, with respect to f_1, f_2, and f_3, since the energy $\mathcal{R}(\phi, \alpha)$ and $\mathcal{L}(\phi)$ are independent of f_1, f_2, and f_3. It can be shown that the energy $\mathcal{E}$ is minimized by

$$f_i = \frac{K_\rho(\mathbf{x}) * [M_i(\phi(\mathbf{x}))I(\mathbf{x})]}{K_\rho(\mathbf{x}) * M_i(\phi(\mathbf{x}))} \qquad i = 1, 2, 3. \quad (7)$$

For fixed f_1, f_2, and f_3, we minimize the energy functional $\mathcal{F}$ with respect to ϕ using the standard gradient descent method and obtain

$$\begin{aligned} \frac{\partial \phi}{\partial t} &= \lambda_1 e_1(\mathbf{x})\delta(\phi(\mathbf{x})) - \lambda_2 e_2(\mathbf{x})(\delta(\phi(\mathbf{x})) - \delta(\phi(\mathbf{x}) - k)) - \lambda_3 e_3(\mathbf{x})\delta(\phi(\mathbf{x}) - k) \\ &\quad + (\nu_1 \delta(\phi(\mathbf{x})) + \nu_2 \delta(\phi(\mathbf{x}) - k)) \operatorname{div}\left(\frac{\nabla\phi(\mathbf{x})}{|\nabla\phi(\mathbf{x})|} \right) \\ &\quad + \mu \left(\nabla^2 \phi(\mathbf{x}) - \alpha(\mathbf{x}) \operatorname{div}\left(\frac{\nabla\phi(\mathbf{x})}{|\nabla\phi(\mathbf{x})|} \right) \right) \end{aligned} \quad (8)$$

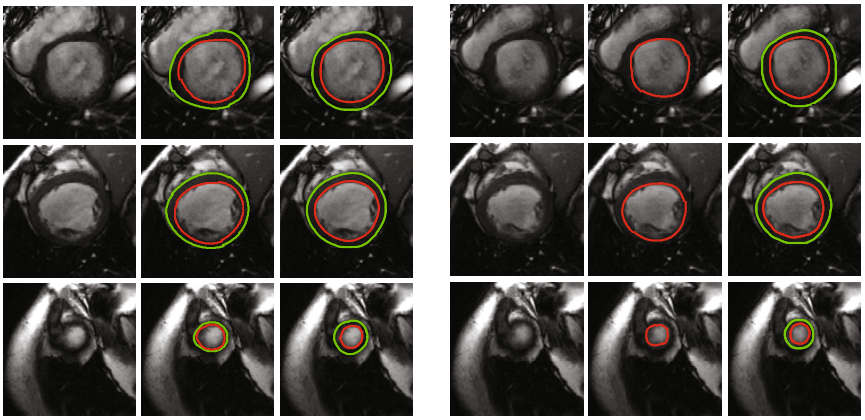

(a) End-diastole **(b)** End-systole

Fig. 1. Results of our method (right column) and ground truth (middle column) for the images from case SC-HF-NI-11 at end-diastole shown in (a) and end-systole in (b). Each row shows one of three slices in an 3D image in the left column.

where $e_i(\mathbf{x}) = \int K_\sigma(\mathbf{y}-\mathbf{x})|I(\mathbf{x}) - f_i(\mathbf{y})|^2 d\mathbf{y}$, $i = 1, 2, 3$ and δ is the Dirac delta function, which is the derivative of H. In the implementation, we use the smooth function $H_\epsilon(x) = [1+(2/\pi)arctan(x/\epsilon)]/2$ to approximate the Heaviside function H with $\epsilon = 1$ and use $\delta_\epsilon(x) = (\epsilon/(\epsilon^2 + x^2))/\pi$ to approximate the Dirac delta function δ as in [8].

3 Results and Discussions

We implemented the level set evolution in Eq. (8) by using standard finite difference scheme as in [8]. Time step $\triangle t$ used in the approximation of temporal derivative is set to $\triangle t = 0.1$. For the data used in this paper, we set the other parameters $\rho = 6$, $\mu = 1$, $\omega = 1$, $\lambda_1 = 0.25$, $\lambda_2 = 1.5$, $\lambda_3 = 0.1$, and $\nu_1 = \nu_2 = 0.05 \times 255 \times 255$.

Our method has been validated on the datasets from the MICCAI challenge on left ventricular segmentation (`http://smial.sri.utoronto.ca/LV_Challenge/Home.html`), which consist of 15 training datasets and 15 validation datasets from a mix of patients and pathologies: healthy (SC-N), hypertrophy (SC-HYP), heart failure with infarction (SC-HF-I), and heart failure with non-ischemic disease (SC-HF-NI). Fig. 1 shows our segmentation results and the ground truth for case SC-HF-NI-11 from the datasets. Note that there is no ground truth provided in the challenge for epicardial contour at end-systole. The obtained contours appear to be quite close to the ground truth.

We compared our segmentation results with the ground truth provided by the MICCAI challenge. The metrics for quantitative evaluation include average

Table 1. Detected and good percentages from the results of different methods

	Training				Validation			
	detected (%)		good (%)		detected (%)		good (%)	
Method	endo	epi	endo	epi	endo	epi	endo	epi
[11]	-	-	-	-	77.8±17.4	85.7±14.1	72.5±19.5	81.1±14.0
[12]	-	-	-	-	99.7±1.4	100	86.4±11.0	94.2±7.0
[13]	-	-	88.4±10.2	92.9±6.5	-	-	92.3±6.1	92.2±5.0
[10]	100	100	96.9±7.6	99.1±3.6	100	100	94.3±9.9	95.6±6.9
Ours	100	100	95.4±5.9	100	100	100	92.8±9.2	96.6±8.1

'-' means no value was reported in this paper.

Table 2. Comparison of contour accuracy in terms of average perpendicular distance and dice coefficient

	Training				Validation			
	APD (mm)		DM		APD (mm)		DM	
Method	endo	epi	endo	epi	endo	epi	endo	epi
[11]	-	-	-	-	2.07±0.61	1.91±0.63	0.89±0.03	0.94±0.02
[12]	-	-	-	-	2.29±0.57	2.28±0.39	0.89±0.03	0.93±0.01
[13]	2.04±0.47	2.35±0.57	0.89±0.04	0.92±0.02	2.04±0.47	2.35±0.57	0.89±0.04	0.92±0.02
[10]	2.09±0.53	1.88±0.40	0.88±0.06	0.93±0.01	2.44±0.62	2.05±0.59	0.88±0.03	0.93±0.02
[14]	2.03±0.34	2.28±0.42	0.90±0.04	0.93±0.02	2.10±0.44	1.95±0.34	0.89±0.04	0.94±0.01
[15]	3.00±0.59	2.60±0.38	0.86±0.04	0.93±0.01	3.00±0.59	2.60±0.38	0.86±0.04	0.93±0.01
Ours	1.82±0.48	1.73±0.43	0.89±0.06	0.94±0.02	1.93±0.37	1.64±0.42	0.89±0.04	0.94±0.02

'-' means no value reported in this paper; in [13] and [15], only one APD and one DM were provided and there was no clarification about the datasets: training, validation, or together.

perpendicular distance (APD) and the dice metric (DM). In the evaluation criterion, if the APD between the ground truth and the detected contour is less than 5mm, the detected contour is graded as *good*. The quotient formed by dividing the number of detected contours by the number of contours from the ground truth is named as *detected percentage*. Division of the number of good contours by the number of detected contours is called the *good percentage*. Although eight methods were evaluated in the challenge, only four provided the detected and good percentage statistic for their methods. These results are shown together with ours in Table 1. We obtained the highest detected percentage, which is exactly 100% both for endocardial (endo) and epicardial (epi) contours on the training and validation datasets. Although the good percentage for our endocardial contours is 1.5 percent lower than the method in [10], we achieved the highest good percentage for the epicardial contour.

Six out of the eight methods in the challenge provided APDs and DMs for their methods, shown in Table 2 together with these measurements obtained using our method. The statistics of the DMs for our method are similar to the other methods in both the training and validation datasets; however, the statistics of the APDs for our method are the smallest: 1.82±0.48 mm and 1.73±0.43 mm for

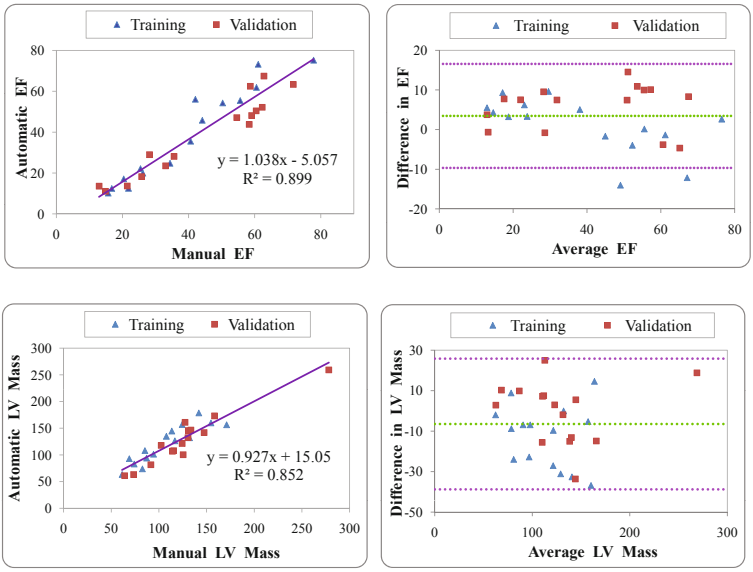

Fig. 2. Regression curves and Bland-Altman plots for EF and left ventricular mass

the training datasets and 1.93±0.37 mm and 1.64±0.42 mm for the validation datasets. This demonstrates that our contours are closest to the ground truth.

Linear regression and Bland-Altman plots for the EF and LV mass obtained by our method are shown in Fig. 2. In this challenge, the linear regression and Bland-Altman plots for EF and LV mass are provided in [10], in which the slope, regression coefficient, and bias on Bland-Altman plots were 1.17, 0.92, -5.22% for EF and 0.77, 0.72, 18.38 grams for LV mass. The corresponding metrics for our method are overall better than those provided in [10].

4 Conclusion

We have proposed a distance regularized two-layer level set model for segmentation of LV from CMR short-axis images. The distance regularization term in our method has a desirable effect of maintaining the smoothly varying distance between the two specified level contours that represent the endocardium and epicardium. We have validated our method on the MICCAI challenge datasets. Quantitative evaluation and comparison with other state-of-the-art methods demonstrate the advantages of our method in terms of segmentation accuracy and the ability to preserve the anatomical geometry of the extracted endocardial and epicardial contours.

References

1. Petitjean, C., Dacher, J.N.: A review of segmentation methods in short axis cardiac MR images. Med. Image Anal. 15(2), 169–184 (2011)
2. Lorenzo-Valdés, M., Sanchez-Ortiz, G.I., Elkington, A.G., Mohiaddin, R.H., Rueckert, D.: Segmentation of 4-D cardiac MR images using a probabilistic atlas and the EM algorithm. Med. Image Anal. 8(3), 255–265 (2004)
3. Zeng, X., Staib, L.H., Schultz, R.T., Duncan, J.S.: Volumetric layer segmentation using coupled surfaces propagation. In: IEEE Conference on Computer Vision and Pattern Recognition (CVPR), pp. 708–715 (1998)
4. Paragios, N.: A variational approach for the segmentation of the left ventricle in cardiac image analysis. Int. J. Comput. Vis. 50(3), 345–362 (2002)
5. Lynch, M., Ghita, O., Whelan, P.F.: Left-ventricle myocardium segmentation using a coupled level-set with a priori knowledge. Comput. Med. Imaging Graph. 30(4), 255–262 (2006)
6. Chung, G., Vese, L.A.: Energy minimization based segmentation and denoising using a multilayer level set approach. In: Rangarajan, A., Vemuri, B.C., Yuille, A.L. (eds.) EMMCVPR 2005. LNCS, vol. 3757, pp. 439–455. Springer, Heidelberg (2005)
7. Li, C., Xu, C., Gui, C., Fox, M.D.: Distance regularized level set evolution and its application to image segmentation. IEEE Trans. Image Processing 19(12), 3243–3254 (2010)
8. Li, C., Kao, C., Gore, J.C., Ding, Z.: Minimization of region-scalable fitting energy for image segmentation. IEEE Trans. Image Processing 17(10), 1940–1949 (2008)
9. Li, C., Xu, C., Gui, C., Fox, M.D.: Level set evolution without re-initialization: a new variational formulation. In: IEEE Conference on Computer Vision and Pattern Recognition (CVPR), pp. 430–436 (2005)
10. Jolly, M.P.: Fully automatic left ventricle segmentation incardiac cine MR images using registration and minimum surfaces. The MIDAS Journal - Cardia MR Left Ventricle Segmentation Challenge (2009)
11. Lu, Y., Radau, P., Connelly, K., Dick, A., Wright, G.: Automatic image-driven segmentation of left ventricle in cardiac cine MRI. The MIDAS Journal - Cardia MR Left Ventricle Segmentation Challenge (2009)
12. Wijnhout, J., Hendriksen, D., Assen, H.V., der Geest, R.V.: LV challenge LKEB contribution: fully automated myocardial contour detection. The MIDAS Journal - Cardia MR Left Ventricle Segmentation Challenge (2009)
13. Constantinides, C., Chenoune, Y., Kachenoura, N., Roullot, E., Mousseaux, E., Herment, A., Frouin, F.: Semi-automated cardiac segmentation on cine magnetic resonance images using GVF-Snake deformable models. The MIDAS Journal - Cardia MR Left Ventricle Segmentation Challenge (2009)
14. Huang, S., Liu, J., Lee, L.C., Venkatesh, S.K., Teo, L.L.S., Au, C., Nowinski, W.L.: Segmentation of the left ventricle from cine MR images using a comprehensive approach. The MIDAS Journal - Cardia MR Left Ventricle Segmentation Challenge (2009)
15. Marák, L., Cousty, J., Najman, L., Talbot, H.: 4D morphological segmentation and the MICCAI LV-Segmentation grand challenge. The MIDAS Journal - Cardia MR Left Ventricle Segmentation Challenge (2009)